Inhibition of COVID-2019 3C-like protease: structure activity relationship using quantum mechanics

Clifford W Fong

Inhibition of COVID-2019 3C-like protease: structure activity relationship using quantum mechanics

Clifford W. Fong
Eigenenergy, Adelaide, South Australia, Australia.
Email: cwfong@internode.on.net

Keywords: COVID-2019; 3C-like protease; inhibition; HOMO-LUMO; quantum mechanics;

Abbreviations: Structure activity relationships SAR, $\Delta G_{desolv,CDS}$ free energy of water desolvation, $\Delta G_{lipo,CDS}$ lipophilicity free energy, CDS cavity dispersion solvent structure of the first solvation shell, Dipole moment DM, Molecular Volume Vol, HOMO highest occupied molecular orbital, LUMO lowest unoccupied molecular orbital, HOMO-LUMO energy gap.

Abstract

The inhibitory efficacy of the 3C-like protease by a series of drugs has been shown to be mainly determined by the HOMO-LUMO energy gap of the inhibitors, with lesser dependencies on the lipophilicity and dipole moment, followed by a smaller dependency on the desolvation of the drugs. As the HOMO-LUMO energy gap of the inhibitors is an inherent chemical reactivity measure, this relationship has predictive implications for the cytotoxicity of inhibitors which may result in undesirable side effects in the body besides the desired inhibition of the target 3C-like protease.

Introduction

The 3C-like protease is an extremely important protease involved in the multiplicative process of Corona viruses, including the deadly Middle East respiratory syndrome coronavirus (MERS-CoV), the SARS-CoV and the COVID-2019. Inhibitors of the 3C-like protease have been successful in treating MERS and SARS and early exploratory studies show that other inhibitors different from those that treated MERS and SARS may be effective in treating COVID-2019. [1-4]

The search for anti-viral drugs that may be effective against COVID-2019 usually can involve searching drug data bases for likely candidates based on generative procedures utilizing crystal structure based binding pocket generation, homology modelling-based generation, and ligand-based generation. The crystal structure of the 3C-like protease is known. [1] Candidate drug docking modeling is often combined with structure activity relationship searching for drugs using molecular properties such as molecular weight, number of rotatable bonds, number of aromatic rings, number of stereocenters, number of hydrogen bond acceptors, number of hydrogen bond donors, the polar surface area, and the MCE-18 medicinal chemistry evolution 2018 descriptor. [1-4]

In this study we use a previously described quantum mechanics model of drugs to investigate structure activity relationships using linear free energy relationships of drug molecular properties and various biological processes such as transport, binding, metabolic, oxidative stress and cytotoxicity studies. There are significant advantages in using quantum mechanics to derive molecular properties of drugs rather than empirical properties such as number of hydrogen bond donors or acceptors, number of aromatic rings or stereocenters, polar surface area etc. By calculating quantum mechanical molecular properties in a water solvent, physico-chemical properties like desolvation, lipophilicity, dipole moment, molecular volume, and the fundamental reactivity properties of highest occupied molecular orbital (HOMO) and lowest unoccupied molecular orbital (LUMO) become available. The HOMO-LUMO energy gap specifies the inherent chemical reactivity of the drug, which is known to be vitally important in the cytotoxicity of the drug and consequent side reactions which are often only found after or during clinical trials. Docking studies give no information about the likely reactivity of the drug in other sites in the body. Desolvation of the drug becomes important as the drug leaves the bulk aqueous cellular environment and starts to interact with the target enzyme in the binding pocket, as described by docking studies. Desolvation, lipophilicity, dipole moment and molecular volume are also critically important in deciding how the drug (intravenous, oral, nasal etc injection) moves from the blood to the cellular target, passing through cell membranes. As many viruses use endocytosis to enter target cells, these molecular properties could also be involved in endocytosis.

Results

We have previously described a model that has been shown to apply to a wide range of drug transport, binding, metabolic and cytotoxicity properties of cells and tumours (Equation 1). The model is based on establishing linear free energy relationships between the four drug properties and various biological processes. Equation 1 has been previously applied to passive and facilitated diffusion of a wide range of drugs crossing the blood brain barrier, [6] the active competitive transport of tyrosine kinase inhibitors by the hOCT3, OATP1A2 and OCT1 transporters, [20] and cyclin-dependent kinase inhibitors and HIV-1 protease inhibitors. [14] The model also applies to PARP inhibitors, the anti-bacterial and anti-malarial properties of fluoroquinolones, and active organic anion transporter drug membrane transport, and some competitive statin-CYP enzyme binding processes. There is strong independent evidence from the literature that $\Delta G_{desolvation}$, $\Delta G_{lipophilicity}$, the dipole moment and molecular volume are good inherent indicators of the transport or binding ability of drugs. [5-22]

Equation 1:

Transport or Binding or Cytotoxicity = $\Delta G_{desolv,CDS}$ + $\Delta G_{lipo,CDS}$ + Dipole Moment + Molecular Volume

Eq 1 uses the free energy of water desolvation ($\Delta G_{desolv,CDS}$) and the lipophilicity free energy ($\Delta G_{lipo,CDS}$) where CDS represents the non-electrostatic first solvation shell solvent properties. CDS may be a better approximation of the cybotactic environment around the drug approaching or within the protein receptor pocket, or the cell membrane surface or the surface of a drug transporter, than the bulk water environment outside the receptor pocket or cell membrane surface. The CDS includes dispersion, cavitation, and covalent components of hydrogen bonding, hydrophobic effects. Desolvation of water from the drug ($\Delta G_{desolv,CDS}$) before binding in the receptor pocket is required, and hydrophobic interactions between the drug and protein ($\Delta G_{lipo,CDS}$) is a positive contribution to binding. The lipophilicity $\Delta G_{lipo,CDS}$ is calculated from the solvation energy in n-octane or n-octanol. In some biological processes, where biological reduction may be occurring, and the influence of molecular volume is small, the reduction potential (electron affinity) has been included in place of the molecular volume. In other processes, the influence of some of the independent variables is small and can be eliminated to focus on the major determinants of biological activity.

We have recently used this model to develop a predictive model of the transport and efficacy of hypoxia specific cytotoxic analogues of tirapazamine and the effect on the extravascular penetration of tirapazamine into tumours. [7] It was found that the multiparameter model of the diffusion, antiproliferative assays IC_{50} and aerobic and hypoxic clonogenic assays for a wide range of neutral and radical anion forms of tirapazamine (TPZ) analogues showed: (a) extravascular diffusion is governed by the desolvation, lipophilicity, dipole moment and molecular volume, similar to passive and facilitated permeation through the blood brain barrier and other cellular membranes, (b) hypoxic assay properties of the TPZ analogues showed dependencies on the electron affinity, as well as lipophilicity and dipole moment and desolvation, similar to other biological processes involving permeation of cellular membranes, including nuclear membranes, (c) aerobic assay properties were dependent on the almost exclusively on the electron affinity, consistent with electron transfer involving free radicals being the dominant species.

Equation 2 also has been shown to apply to the inhibition of acetylcholinesterase by Donepezil analogs. [5] Eq 2 also applies to triple negative breast and ovarian cancers where transient and stable free radicals are involved in the cytotoxic oxidative stress processes. The electron affinity of the various drugs, along with the water desolvation, lipophilicity and dipole moment, has been shown to be an important predictor of cytotoxic efficacy. [10-12] In our recent study of ORAC and CellROX free radical anticancer drugs and oxidative stress in colorectal cancer cells [8,9] we found that eq 2 was also applicable.

The antioxidant capacity (or chemical reactivity) of the drugs can be assessed by the HOMO-LUMO energy gap, since we have recently shown that this gap is linearly related to the LD_{50} toxicity of various drugs which are involved in oxidative stress processes in some cancers. [8,12-13] Eq 2 can then be represented by including the HOMO-LUMO energy gap instead of the molecular volume. In particular, we have recently examined the mechanism and structure activity relationships of lipid peroxidation of cell membranes and brain protection for cerebral ischemia by Edaravone and Edaravone analogs [21] and improved Edaravone delivery to the brain and crossing the blood brain barrier [22] using variants of eq (2)

Equation 2.

Oxidative Stress or Toxicity = $\Delta G_{desolv,CDS}$ + $\Delta G_{lipo,CDS}$ + Dipole Moment + (HOMO–LUMO)

Evaluation methodology

Given the successful transport, binding or cytotoxicity model as described by eq 1 and 2 for wide range of drugs, the method used was to calculate the molecular parameters for the 43 inhibitors used on the 3C-like protease by Lin [3] as shown in Figure 1: (1) the free energy of water desolvation ($\Delta G_{desolv,CDS}$), (2) the lipophilicity free energy ($\Delta G_{lipo,CDS}$) in n-octane, (3) the dipole moment in water, (4) the molecular volume in water, and (5) HOMO, (6) LUMO or (7) HOMO-LUMO energy gap in water. These values are shown in Table 1. These independent variables values have similar magnitudes so that the coefficients in the multiple linear regression equations can be directly compared to gauge the relative magnitudes of inhibitory sensitivity of these molecular variables.

Stepwise multiple regression was then applied to seek out which of the seven drug molecular properties had the largest most significant effect on the inhibition in Table 1. Equation 3 below shows the most statistically significant relationship found after testing against all independent variables in a stepwise fashion. Three inhibitors numbers 1,22 and 43 were excluded as outliers from eq 3 (including these three inhibitors resulted in a Standard Error of the Estimate SEE of 0.469, F of 3.33 and significance of 0.020, a much weaker relationship).

Eq 3 Inhibition of 3C-like protease pIC_{50} for 40 compounds from [3] was:

pIC_{50} = 0.05$\Delta G_{desolv,CDS}$ - 0.11$\Delta G_{lipo,CDS}$ - 0.08Dipole Moment – 0.23(HOMO-LUMO) + 6.63

Where R^2 = 0.382, SEE = 0.39, SE($\Delta G_{desolvCDS}$) = 0.04, SE($\Delta G_{lipoCDS}$) = 0.04, SE(Dipole Moment) = 0.025, SE(HOMO-LUMO) = 0.08, F=5.42, Significance=0.0017

It can be seen that strongest relationship was between pIC_{50} and $\Delta G_{lipo,CDS,}$ the Dipole Moment and the (HOMO-LUMO) energy gap, as the P values for the coefficients was 0.015, 0.004 and 0.012 respectively compared to the P value of 0.263 for the $\Delta G_{desolv,CDS}$ coefficient. Eq 3 can be modified to delete the $\Delta G_{desolv,CDS}$ term, which gives a slightly stronger correlation SEE 0.39, F 6.73, significance 0.001. However it is clear that eq 3 is statistically strong, even though the effect of desolvation is less precise than the other independent variables.

Discussion

The inhibition of 3C-like protease shown in eq 3 demonstrates that the HOMO-LUMO energy gap is the dominant factor is determining the inhibitory efficacy. Lipophilicity and the dipole moment are roughly about a half to a third less influential than the HOMO-LUMO energy gap, and water desolvation is the lesser influential factor being about a fifth of that of the HOMO-

LUMO gap. The HOMO-LUMO gap of the inhibitors will also be influential in determining drug cytotoxicity involved in predicting drug side effects elsewhere in the body. [8,12,13]

We have recently shown that inhibition of acetylcholinesterase by Donepezil analogs is strongly dependent upon the LUMO with minor dependencies on desolvation, lipophilicity and dipole moment. [5] Equation 1 has been previously applied to passive and facilitated diffusion of a wide range of drugs crossing the blood brain barrier, [6] the active competitive transport of tyrosine kinase inhibitors by the hOCT3, OATP1A2 and OCT1 transporters, [20] and cyclin-dependent kinase inhibitors and HIV-1 protease inhibitors. [14]

It is noted that this study uses all the data (with 3 outliers) without any other statistical manipulation such as dividing the data into arbitrary training and test data sets and using algorithmic improvement methods.

Lin [3] has shown that a SAR based on comparative molecular field analysis (CoMFA) and comparative molecular similarity indices analysis (CoMSIA) for these 43 drugs describes the inhibitory behaviour well. The SAR data is backed up by docking studies and molecular dynamics study. However the quantitative SAR uses a separate training and test data set separation to optimize that SAR, which may introduce algorithmic overfitting artifacts as well as sampling errors when choosing the particular training and test sets. The inherent experimental error in the pIC_{50} data is still the same in both training and test sets. A major problem in all (biological) test data is the inherent error which is best minimized by using the data from the same laboratory and in the same study, which occurs in Lin's study. [3] Studies of test data from many different literature studies may have very large discrepancies due to different laboratory conditions and unknown and varying experimental errors. The CoMFA is a molecular field-based, *alignment-dependent*, ligand-based method. The method mostly focuses on ligand properties like steric and electrostatic ones, and the resulting favorable and unfavorable receptor-ligand interactions using a force field.

The current methodology employed in this study has significant advantages over the COMFA methodology.

Conclusions

The inhibitory efficacy of the 3C-like protease by a series of drugs has been shown to be mainly determined by the HOMO-LUMO energy gap of the inhibitors, with lesser dependencies on the lipophilicitiy and dipole moment, followed by a smaller dependency on the desolvation of the drugs. As the HOMO-LUMO energy gap of the inhibitors is an inherent chemical reactivity measure, this relationship has predictive implications for the cytotoxicity of inhibitors which

may result in undesirable side effects in the body besides the desired inhibition of the target 3C-like protease.

Experimental Methods

All calculations were carried out using the Gaussian 09 package. Energy optimizations were at the DFT/B3LYP/6-31G(d,p) (6d, 7f) or DFT/B3LYP/3-21G (for larger molecules) level of theory for all atoms. Selected optimizations at the DFT/B3LYP/6-311+G(d,p) (6d, 7f) level of theory gave very similar results to those at the lower level. Optimized structures were checked to ensure energy minima were located, with no imaginary frequencies. Energy calculations were conducted at the DFT/B3LYP/6-31G(d,p) (6d, 7f) for neutral and cationic compounds with optimized geometries in water, using the IEFPCM/SMD solvent model. With the 6-31G* basis set, the SMD model achieves mean unsigned errors of 0.6 - 1.0 kcal/mol in the solvation free energies of tested neutrals and mean unsigned errors of 4 kcal/mol on average for ions. [23] The 6-31G** basis set has been used to calculate absolute free energies of solvation and compare these data with experimental results for more than 500 neutral and charged compounds. The calculated values were in good agreement with experimental results across a wide range of compounds. [24,25] Adding diffuse functions to the 6-31G* basis set (ie 6-31+G**) had no significant effect on the solvation energies with a difference of less than 1% observed in solvents, which is within the literature error range for the IEFPCM/SMD solvent model. HOMO and LUMO calculations included both delocalized and localized orbitals (NBO).
It is noted that high computational accuracy for each species in different environments is not the focus of this study, but comparative differences between various species is the aim of the study.

References

[1] A Zhavoronkov, V Aladinskiy, A Zhebrak, B Zagribelnyy, V Terentiev, DS Bezrukov, D Polykovskiy, R Shayakhmetov, A Filimonov, P Orekhov, Y Yan, O Popova, Q Vanhaelen, A Aliper, Ivanenkov, Potential COVID-2019 3C-like Protease Inhibitors Designed Using Generative Deep Learning Approaches, doi.org/10.26434/chemrxiv.11829102.v2

[2] M Macchiagoden, M Pagliai, P Procacci Inhibition of the Main Protease 3CLPro of the Coronavirus Disease 19 via Structure-Based Ligand Design and Molecular Modeling, ArXiv:2020.09937v2, 2 Mar 2020

[3] F Lin, XM Fu, C Wang, SY Jiang, JH Wang, SW Zhang, L Yang, Y Li, QSAR, Molecular Docking and Molecular Dynamics of 3C-like Protease Inhibitors, Acta Phys. Chim. Sin. 2016, 32, 2693-2708

[4] V Kumar, KP Tan, YM Wang, SWei Lin, PH Liang, Identification, synthesis and evaluation of SARS-CoV and MERS-CoV 3C-like protease inhibitors, Bioorg. Med. Chem. 2016, http://dx.doi.org/10.1016/j.bmc.2016.05.013

[5] CW Fong, Comparison of choline blood brain barrier and neuronal transport and anticholinesterase inhibitory properties of potential cationic Alzheimers disease drugs**,** HAL Archives, 2020, https://hal.archives-ouvertes.fr/hal-

[6] CW Fong, Permeability of the Blood–Brain Barrier: Molecular Mechanism of Transport of Drugs and Physiologically Important Compounds, J Membr Biol. 2015, 248,651-69.

[7] CW Fong, The extravascular penetration of tirapazamine into tumours: a predictive model of the transport and efficacy of hypoxia specific cytotoxic analogues and the potential use of cucurbiturils to facilitate delivery, Int J Comput Biol Drug Design. 2017, 10, 343-373
[8] CW Fong, Screening anti-colorectal cancer drugs: free radical chemotherapy, HAL Archives, 2019, https://hal.archives-ouvertes.fr/hal-02271521v1
[9] CW Fong, Free radical anticancer drugs and oxidative stress: ORAC and CellROX-colorectal cancer cells by quantum chemical determinations, HAL Archives, 2018 https://hal.archives-ouvertes.fr/hal-01859315v1.
[10] CW Fong, The role of free radicals in the effectiveness of anti-cancer chemotherapy in hypoxic ovarian cells and tumours, HAL Archives, 2018, hal-01659879, https://hal.archives-ouvertes.fr/hal-01659879v2
[11] CW Fong, Free radicals in chemotherapy induced cytotoxicity and oxidative stress in triple negative breast and ovarian cancers under hypoxic and normoxic conditions, HAL Archives, 2018, https://hal.archives-ouvertes.fr/hal-01815246v1
[12] CW Fong, Role of stable free radicals in conjugated antioxidant and cytotoxicity treatment of triple negative breast cancer, HAL archives 2018, https://hal.archives-ouvertes.fr/hal-01803297
[13] CW Fong, Toxicology of platinum anticancer drugs: oxidative stress and antioxidant effect of stable free radical Pt-nitroxides, HAL Archives, 2019, hal-01999011, version 1**,** https://hal.archives-ouvertes.fr/hal-01999011v1
[14] CW Fong, The effect of desolvation on the binding of inhibitors to HIV-1 protease and cyclin-dependent kinases: Causes of resistance, Bioorg Med Chem Lett. 2016, 26, 3705–3713.
[15] CW Fong, Physiology of ionophore transport of potassium and sodium ions across cell membranes: Valinomycin and 18-Crown-6 Ether. Int J Comput Biol Drug Design 2016, 9, 228-246.
[16] CW Fong, Statins in therapy: Understanding their hydrophilicity, lipophilicity, binding to 3-hydroxy-3-methylglutaryl-CoA reductase, ability to cross the blood brain barrier and metabolic stability based on electrostatic molecular orbital studies. Eur J Med Chem. 2014, 85, 661-674
[17] CW Fong, Predicting PARP inhibitory activity – A novel quantum mechanical based model. HAL Archives. 2016, https://hal.archives-ouvertes.fr/hal-01367894v1.
[18] CW Fong, A novel predictive model for the anti-bacterial, anti-malarial and hERG cardiac QT prolongation properties of fluoroquinolones, HAL Archives. 2016, https://hal.archives-ouvertes.fr/hal-01363812v1.
[19] CW Fong, Statins in therapy: Cellular transport, side effects, drug-drug interactions and cytotoxicity - the unrecognized role of lactones, HAL Archives, 2016, https://hal.archives-ouvertes.fr/hal-01185910v1.
[20] CW Fong, Drug discovery model using molecular orbital computations: tyrosine kinase inhibitors. HAL Archives, 2016, https://hal.archives-ouvertes.fr/hal-01350862v1
[21] CW Fong, Mechanism, structure activity relationships of lipid peroxidation of cell membranes and brain protection for cerebral ischemia by Edaravone and Edaravone analogs – a quantum mechanical study, HAL Archives, 2019, hal-02428109, https://hal.archives-ouvertes.fr/hal-02428109v1
[22] CW Fong, Improved Edaravone delivery to the brain and crossing the blood brain barrier: using quantum mechanics, HAL Archives, 2019, hal-02292553v2, https://hal.archives-ouvertes.fr/hal-02292553v2

[23] AV Marenich, CJ Cramer, DJ Truhlar, Universal Solvation Model Based on Solute Electron Density and on a Continuum Model of the Solvent Defined by the Bulk Dielectric Constant and Atomic Surface Tensions, J Phys Chem B, 2009, 113, 6378 -96
[24] S Rayne, K Forest, Accuracy of computational solvation free energies for neutral and ionic compounds: Dependence on level of theory and solvent model, Nature Proceedings, 2010, http://dx.doi.org/10.1038/npre.2010.4864.1.
[25] RC Rizzo, T Aynechi, DA Case, ID Kuntz, Estimation of Absolute Free Energies of Hydration Using Continuum Methods: Accuracy of Partial Charge Models and Optimization of Nonpolar Contributions, J Chem Theory Comput. 2006, 2, 128-139

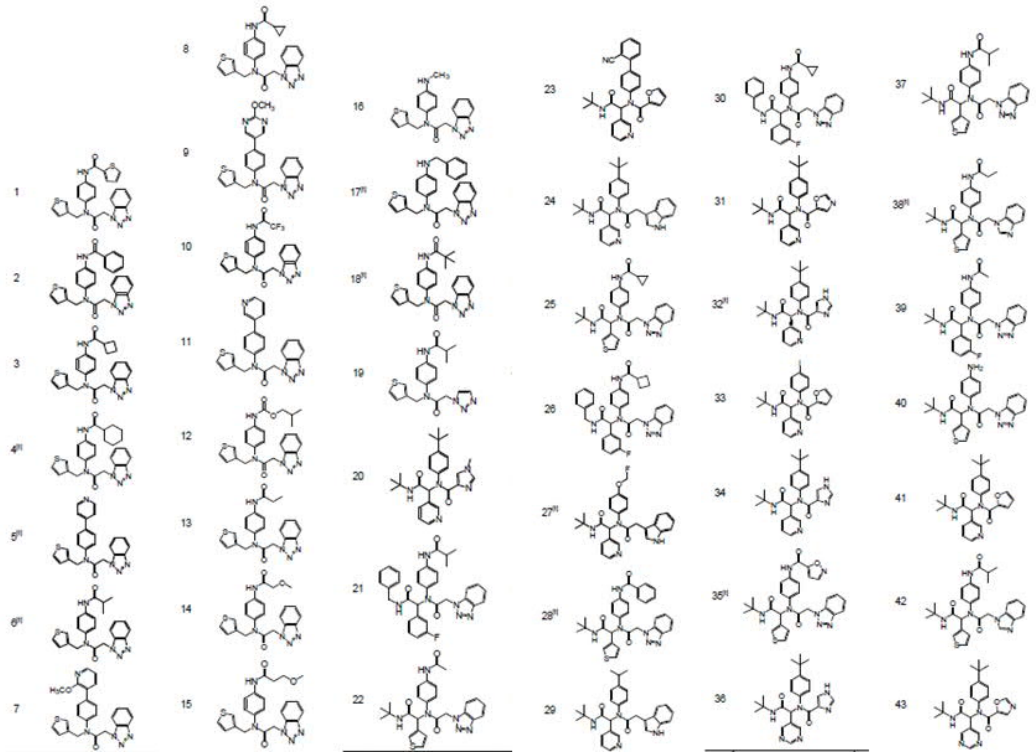

Figure 1. 3C-like protease inhibitors (taken from Lin [3])

	pIC_{50}	**$\Delta G_{desolv,CDS}$** kcal/mol	**$\Delta G_{lipo,CDS}$** kcal/mol	**Dipole Moment** D	**Molec Volume** cm^3/mol	**HOMO** eV	**LUMO** eV	**HOMO-LUMO** eV
1	6.48	-7.89	-9.42	9.16	312	-5.82201	-1.52333	4.29868
2	6.39	-8.21	-10.32	8.69	301	-5.89276	-1.2474	4.645361
3	5.92	-7.4	-9.57	8.7	278	-5.85221	-1.24604	4.606175
4	5.92	-7.53	-10.36	8.7	336	-5.8514	-1.24577	4.605631
5	5.82	-6.26	-8.99	10.2	298	-6.33223	-1.31434	5.017893
6	5.8	-7.83	-8.5	8.77	327	-5.82827	-1.24495	4.583317
7	5.77	-7.92	-9.87	12.47	322	-6.22855	-1.85477	4.373785
8	5.72	-7.25	-9.29	8.74	330	-5.85412	-1.24604	4.60808
9	5.7	-6.36	-8.78	11.18	313	-6.05467	-1.22264	4.832035
10	5.66	-8.77	-6.5	8.19	283	-6.0114	-1.26291	4.748494
11	5.62	-5.82	-8.89	8.25	293	-6.11263	-1.22182	4.890813
12	5.55	-8.85	-8.56	8.58	338	-5.88187	-1.24604	4.635836
13	5.51	-7.44	-8.34	8.68	223	-5.82418	-1.24495	4.579235
14	5.51	-8.31	-7.66	9.58	334	-5.8631	-1.24604	4.61706
15	5.43	-8.34	-8.24	8.06	282	-5.84731	-1.24577	4.601549
16	5.32	-5.65	-7.08	9.55	278	-4.97871	-1.23488	3.743827
17	5.28	-7.04	-9.94	9.34	342	-5.03885	-1.23515	3.803693
18	5.06	-7.09	-7.78	9.63	275	-4.93517	-1.23406	3.701104
19	4.8	-8.6	-6.98	11.52	273	-5.85793	-0.64547	5.212459
20	5.89	-10.91	-10.91	11.14	393	-2.51466	-0.40791	2.106753
21	5.82	-10.59	-12.1	15.69	366	-2.95005	-0.69472	2.255331
22	5.74	-10.49	-8.37	16.18	375	-6.07317	-1.19461	4.878567
23	5.66	-11.55	-9.29	10.3	395	-6.32434	-1.48632	4.838021
24	5.66	-11.83	-11.2	9.24	395	-5.57628	-0.83867	4.737609
25	5.57	-10.32	-9.85	16.16	318	-6.06692	-1.19488	4.872036
26	5.47	-11.49	-13.13	16.29	437	-6.10284	-1.19896	4.903875
27	5.41	-11.77	-9.61	8.3	349	-5.58417	-0.8501	4.734072
28	5.38	-11.38	-10.9	16.19	395	-6.14556	-1.19624	4.949319
29	5.16	-11.43	-11.22	9.19	382	-5.57656	-0.83922	4.737337
30	5.15	-11.24	-12.92	16.37	437	-6.07753	-1.19869	4.878839
31	5.07	-7.38	-6.88	10.7	348	-6.4604	-1.5949	4.865506
32	5.03	-8.18	-9.45	8.43	328	-6.18093	-0.79105	5.389881
33	5.02	-7.78	-7.77	8.47	305	-6.40462	-1.54483	4.859791
34	4.95	-8.18	-9.45	8.43	328	-6.18093	-0.79105	5.389881
35	4.83	-10.79	-9.11	15.12	344	-6.18393	-1.78484	4.399092
36	4.81	-7.25	-10.54	10.65	340	-6.26012	-1.11624	5.143884
37	4.76	-10.85	-9.62	15.11	371	-6.05739	-1.20168	4.855709
38	4.74	-10.59	-12.54	17.6	371	-6.06664	-0.61744	5.449203
39	4.73	-11.32	-7.76	14.81	311	-4.79367	-1.19787	3.595794
40	4.66	-8.65	-7.28	15.56	298	-5.32321	-1.1957	4.127516
41	4.45	-10.33	-8.42	10.2	328	-6.25577	-1.12549	5.130278
42	4.28	-11	-13.03	16.85	328	-6.03426	-0.54097	5.493286
43	4.25	-6.01	-7.34	8.41	371	-6.48598	-1.63272	4.85326

Table 1. Molecular properties of inhibitors of C3-like proteases (see Figure 1 for inhibitor structures)